

# Measuring Facial Grimacing for Quantifying Patient Agitation in Critical Care

Pierrick Becouze<sup>1</sup>, Christopher E. Hann<sup>2</sup>, J. Geoffrey Chase<sup>3</sup>, Geoffrey M. Shaw<sup>4</sup>

Department of Mechanical Engineering

University of Canterbury

Private Bag 4800

Christchurch

New Zealand

Email: [Chris.Hann@canterbury.ac.nz](mailto:Chris.Hann@canterbury.ac.nz)

---

<sup>1</sup> Research Assistant, Dept. of Mech. Eng, Centre for Bio-Engineering

<sup>2</sup> Research Associate, New Zealand Science and Technology Postdoctoral Fellow, Dept. of Mech. Eng,  
Centre for Bio-Engineering

<sup>3</sup> Assoc. Prof./ Reader, Dept. of Mech. Eng, Centre for Bio-Engineering

<sup>4</sup> Clinical Intensivist, Department of Intensive Care, Christchurch Hospital, Christchurch, New Zealand

## **ABSTRACT**

The effective delivery of sedation in critical care relies primarily on an accurate and consistent measure of a patient's agitation level. However, current methods for assessing agitation are subjective and prone to error, often leading to over sedation or cycles between agitation and oversedation. This paper builds on previous work developing agitation sensors based on heart rate and blood pressure variability, and overall whole body motion. In this research, the focus is on real-time measurement of high resolution facial changes that are observed to occur in agitation. An algorithm is developed that measures the degree of facial grimacing from a single digital camera. The method is demonstrated on simulated patient facial motion to prove the concept. A consistent measure is obtained that is robust to significant random head movement and compares well against visual observation of different levels of grimacing. The method provides a basis for clinical validation.

*Keywords*—Agitation Sensor, Sedation, Critical Care, Digital Camera, Image Processing, Facial Grimacing

## **1. Introduction**

In critical care many patients are mechanically ventilated and sedated for relatively long periods. Sedative dosing is thus primarily titrated to provide a minimum level of unconsciousness to facilitate recovery while also minimizing patient agitation.

Patients commonly experience agitation in the ICU as a result of invasive life support systems, combined with their disease, injury and environment. Agitation reduces the ability of the patient to recover, thus potentially increasing length of stay and cost. Other potential risks include self extubation, removal of catheters and lines, and injury to staff [1].

To reduce agitation, patients are commonly sedated by intermittent bolus or continuous infusion of sedative and analgesic drugs [1,2]. Therefore, effective delivery of sedation is fundamental in the ICU, and is the basis for providing comfort and relief to the critically ill. However, there is no accepted gold standard for measuring agitation and current methods are subjective and prone to error. This subjective level of assessment can lead to over sedation, variable delivery of sedative, and increased cost and prolonged length of stay [1, 3, 4].

A quantitative, consistent agitation sensor based on observed clinical behaviour could enable more effective sedation administration [5-7]. In previous work, agitation sensors based on blood pressure and heart rate variability [8] and digital imaging of whole body motion [9], have been developed and validated [10]. Furthermore, significant potential improvements in agitation and sedation management have been shown using clinically validated model simulation to examine automated or semi-automated sedative infusion methods using agitation feedback [6,7]. These control methods were based on a physiological model of agitation and sedation pharmacodynamics [5,6,11,12].

This paper extends the agitation sensor by creating a measure of the degree of facial grimacing and head motion. These motions are known to be an important indicator of agitation in the critically ill [13-15], offering the potential to provide earlier and/or consistent quantitative detection of agitation. Note that the whole body

movement approach [9,10] is limited to measuring essentially average body motion, and has relatively low resolution of the head and face. Since the camera takes images of the whole body there is an inherent perspective distortion due to the oblique viewing angle, potentially reducing the resolution of motion detection and measurement. Furthermore, in the case of paraplegic patients [16], whole body movement is not available, significantly hindering the use of [9,10]. Facial expression is also particularly important for measuring pain in pediatrics [17-20], is one of the key elements of Behavioural Pain Assessment [21] and is a significant part of pain measurement in general [22-25].

In this research, the camera is focused primarily on the head and face rather than an overall view of the whole body [9,10]. This approach provides potentially much greater facial resolution and thus the ability to detect subtle facial changes. More specifically, during, and prior to, agitation, there can be significant head movement and facial grimacing. Thus, dynamically changing features must be tracked and measured in real time, regardless of head movement. Thus, this problem presents two main problems: 1) tracking the head during potentially vigorous patient motion, and 2) measuring facial grimacing and motion in that tracked facial region. Both tasks must occur in clinical real time, implying the need for computationally efficient, as well as accurate, methods.

A number of facial recognition and tracking algorithms exist (e.g. [26-31]), However these algorithms usually deal with either the detection and tracking of static facial features [28], or purely describe qualitatively overall facial changes [31]. Neither task is typically done within the real time constraints needed for critical care, which are on the order of 1-5 times per second to effectively track changes [9,10].

The goal in this paper is to develop methods for detecting and quantifying dynamic feature change related to facial grimacing, independent of head movement.

## **2. Methodology**

The primary focus is on calculating a view independent measure of facial grimacing. Therefore, the head must first be tracked, specific regions of the face need to be located and a measure of grimacing based on image properties must be developed. The methodology for this approach is presented in a general manner but is explained in terms of two specific simulated examples. The first example concentrates on the tracking of the dot with no facial expression. The second example demonstrates the full development of a measure of facial grimacing independent of the camera viewing angle. The section is organized by starting with a description of the experimental setup, followed by a step by step overview of the proposed algorithm. Each step of the algorithm is then described and explained in more detail.

### **Experimental Setup**

Video broadly imitating the full possible range of facial grimacing of a patient in critical care provide proof of concept data, using a Canon IXUS 40 digital camera. The digital camera is focused approximately normal to the patient's face, as shown in Figure 1. The images cover a range of grimacing from calm to exaggerated expression.

Camera details include:

- Video format: '.avi'
- Resolution of video frame: 320\*240
- Frame/ Second: 30
- Video Compression: 'MJPG'
- Video frames colour: RGB

The video simulates:

1. A patient moving head with no expression
2. A patient moving head and grimacing

Each frame is stored as a jpeg file and processed frame-by-frame using MATLAB 7.1.

MATLAB is used to develop the algorithms, but in a manner that would generalise to an implemented real-time system.

## **Overview of proposed algorithm**

The algorithm has five fundamental processing steps:

### **Step 1. Detect head position**

A reference point(s) is placed on the patient (e.g. black dot on forehead or ventilator tube) to enable a simple and efficient automated method for consistently locating a known location on the head.

### **Step 2. Put boundary around face**

To ensure accuracy in isolating the required regions of the face, the boundary contour surrounding the face is extracted. The results segregate the portion of the face visible to the camera for processing.

### **Step 3. Segment the face**

The face is segmented into pre-determined sections based on regions that are clinically claimed to be most representative of the grimacing evidenced in patient agitation. These regions are clinically selected, but can be arbitrarily changed based on new clinical input.

### **Step 4. Evaluate grimacing**

Each pre-determined region of the face in step 3 is analysed to measure the degree of facial change relative to a static, resting case calibration with no appreciable facial expression. All information including the magnitude and frequency of head movement, grimacing and facial features from step 4 are combined to create a metric reflecting the amount of change.

### **Step 5. Compute agitation measure**

Combines the information from step 4 with other heart rate or blood pressure measurements as in [8] to compute an overall agitation measure that can be used as a feedback control quantity to provide more effective sedation [6,7].

## **Reference point tracking (Step 1)**

To easily determine head position, a white marker containing a black dot is placed on the forehead, as shown in Figure 2. The aim is to detect the marker in the first frame and follow it in the following frames. In a critical care setting a patient usually has a ventilator and/or tubes from the mouth so that several artificial points could be placed. These markers would be permanent, except during the possibility of extreme patient agitation where they may grab the ventilator and/or tubes and attempt to remove them from the mouth. However, if a marker was dislodged this would be easily automatically detected as missing from the image and could then be placed back on the patient by clinical staff.

To detect the dot, the RGB image is first converted to greyscale. For computational efficiency and improved accuracy, a rectangular area is then placed around the dot such that for any position of the head, the dot always stays within this area, as shown in Figure 2(a). Thus, only this limited area has to be processed to find the dot position. This area would have to be pre-set by the nursing staff for a few patients and/or set relatively large.

The greyscale image of the rectangular area is smoothed by replacing each pixel intensity by the average of itself and its 8 neighbouring pixel intensities. This smoothing is applied two times and the rectangular area is then normalized by re-scaling the pixels from 0 to 10. Specifically, let  $\bar{I}_{min}$  and  $\bar{I}_{max}$  be the minimum and maximum intensities respectively. The new-scaled intensity,  $\bar{I}$ , corresponding to  $I$  is defined:

$$\bar{I} = \frac{10I}{I_{max} - I_{min}} - \frac{10I_{min}}{I_{max} - I_{min}} \quad (1)$$

Using Equation (1) it is easily shown that  $\bar{I}_{min} = 0$  and  $\bar{I}_{max} = 10$ . This scaling enables a consistent threshold level to be chosen independent of changes in

brightness, which allows pixels above this threshold to be readily deleted. Figure 2(b) shows Figure 2(a) after this process.

Once thresholding is done, the rectangle is processed to eliminate elements that are not the required dot. Figure 3 shows four cases representing each possible outcome. The methods keep only black objects surrounded by white, which is precisely the property of the artificially placed reference point. The first step takes the complement image and the second makes all white areas touching a border black. In cases (a), (b) and (c); every unwanted area is deleted leaving only the white dot. Nevertheless, if there is any other black object circled by white, it will remain, as shown in Figure 3 (d).

For Figure 3(d), this process requires a correct initial position of the black dot. Thus, for the first frame, an upper and lower bound  $N_{min}$  and  $N_{max}$  is placed on the number of pixels making up the black dot. All regions not within the  $N_{min}$ - $N_{max}$  pixel bound are deleted, leaving the required black dot. This method will leave regions that have a similar number of pixels to the black dot. However this case should be rare in a controlled clinical environment. Finally, by taking an average of all the pixels in the black dot, the centre of the black dot in Figure 2 (a) is found.

For subsequent frames, the correct dot is identified by requiring it to be within a predefined tolerance from the black dot in the previous frame. This tolerance is chosen to be +4 and -4 pixels given the 30 fps image rate. For faster computation, the rectangle area can also be reduced once the dot in the first frame is found.

## **Extracting boundary contour of face (Step 2)**

With only one dot to act as a landmark point, the location of this dot is not sufficient to consistently enable the placement of a rectangle around the cheek region or any other region restricted to certain areas on the face. For significant rotations of the head, part of the cheek on one side can disappear and the size of such regional rectangles will change significantly. To correct this error would require either more artificial points to be placed on the face or natural facial features to be tracked. In a hospital environment, it is undesirable and impractical to require too many artificial points to be placed on a patient's face. Thus, a form of the latter option is chosen.

Since the boundary contour of the visible part of the face remains largely unchanged during facial grimacing, a method for tracking the contour is developed. Common methods for tracking face contour use snakes with gradient [30] or colour information [27] as exterior forces on the snakes to aid the process. However, in this application thousands of frames need to be tracked in real time. Thus, the method of snakes would be computationally heavy. In addition, that high a level of accuracy is not required, as only the essential facial outline is needed. Therefore, a simpler computationally efficient method is used based on skin colour segmentation and constrained by a restriction on movement between frames.

Note that the case simulated in this paper is a conservative choice where only one artificial landmark point is used. In practice, with tubes and a ventilator on a patient, many more artificial landmark points would be available, making the job of motion tracking and identifying facial regions simpler. Any tubes crossing the boundary could be accounted for in an initialization which would incorporate user input if required. The position of the tubes would be known throughout time by tracking the artificial landmark points.

However, if there is a sufficient number of landmark points such that facial regions of interest can be easily located, a boundary algorithm may not be required. This possibility is left to future clinical trials. Importantly, the methodology in this paper is designed to track any number of landmark points and utilize the boundary of the face as required. Also note that a longer term goal is to apply the method in the general wards, where there are less artificial landmark objects/points available as patients are less likely to be on a ventilator or have tubes.

### **2.4.1 Skin recognition**

Extraction of the contour uses a skin hue property to detect the edge of the face. Specifically, the R/G ratio of the intensity value on the red (R) channel to the intensity on the green (G) channel can be used to represent skin [32,33]. Using the position of the dot to get a sample of the skin hue on the forehead, it is thus possible to detect skin on the face of a specific patient. Note that the studies of [32,33] successfully detect skin on a very large data set containing a wide number of skin types. In critical care patients there is the possibility of paler skin due to their severe illness. However, measurements have shown that paler skin has almost the same chromaticity as yellowish or dark skin [34-36] thus presenting no further significant difficulty. Skin can also show up more white than usual due to changes in light, but this effect is normalized out by taking colour ratios and is shown to have minimal effect on skin detection [36-38].

Figure 4 shows examples of detecting skin based on deleting pixels that have an intensity ratio R/G greater than a specified tolerance of the sample skin intensity.

However, as can be seen in Figure 4, the face is not precisely defined and requires further processing to accurately isolate areas associated with grimacing. In addition, bandages or other coverings would hide skin, although such areas would not contribute to agitation detection either.

### **2.4.2 Contour extraction**

Thresholding of the R/G ratio can be used to approximate the boundary of the face separating skin from non-skin. However, this method does not always accurately detect all parts of the boundary. Therefore an initial contour extraction is done on the first image of the sequence. This contour is found by using the R/G ratio to find all the discrete boundary points on the face, thus forming the contour. This contour must then be checked by the user before the algorithm proceeds, making corrections if necessary.

This initialization is used to assist in extracting the contour in future frames. The number of pixels defining the facial contour curve is set to 50 equally spaced points (in Euclidean distance) around the perimeter of the contour. This number is arbitrary, but provides enough segments to adequately define the fundamental visible face in an image. More or less points might be equally effectively used.

The amount of pixel movement between frames at 30 fps is relatively small, and can be bounded above by a predefined tolerance  $\delta$ . Therefore, each new contour will lie inside an envelope around the previous contour. In particular, for every point on the previous contour, the boundary of the new contour is searched for along the line

segment perpendicular to the tangent of the curve, with a length determined by the pre-defined tolerance  $\delta$ . Figure 5, shows this line segment in an example image.

The goal is to detect which point along the line A to B best meets the criteria for the border of the face. The gradient of the red, green and blue intensities between points A and B would appear to be a simple way of doing this task. However, there is not always a clearly defined boundary, which can result in no significant change in the gradient across the boundary leading to potentially false points being chosen. A more robust solution uses the ratio of the red and green signals, which is shown in Figure 6.

When the ratio of the red and green is above a predefined threshold, which is chosen as 1.18 in Figure 6, it is considered to be skin. The first point of the segment that is above the threshold is defined as the boundary. If no such point is found, no point is stored. The resulting gaps left in the curve are then linearly interpolated using equally spaced points.

For additional robustness, a simple learning system can be used. For every tracked position of the black dot, the boundary contour can be stored. Thus, when the head comes back to a point close to a known position, the corresponding stored contour can be used instead of re-calculating.

### **Measuring dynamic facial grimacing (Steps 3-4)**

During grimacing, extra wrinkles appear on the face and similarly for agitation evidenced by biting or chewing the endo-tracheal tube. These wrinkles occur dynamically and can be detected as extra edges on the image. Since edges are largely

unaffected by the rotation of the head and different lighting conditions, edge detection was chosen as the basis for defining a grimacing measure.

To accomplish this task in a computationally efficient manner, a high-pass filter is applied on an extracted region of the image to locate the edges corresponding to the wrinkles. The specific filter looks for zero crossings after filtering the image with a Laplacian of the Gaussian filter [39].

For better consistency, this high-pass filter is applied only where the wrinkles are most likely to be located. Specifically, from above the eyebrows to the sides of the mouth, as seen for a series of facial grimaces in Figures 9-10. This approach saves computation by examining areas of known occurrence. It also provides a more dynamic measure by ignoring areas where little change is likely to occur.

The overall approach first finds the facial contour. The face is then segmented from above the eyebrows to below the mouth. The head tracking dot position is used to find these regions relative to the dot's location and provide a consistent facial segmentation.

Next, a sequence of initialization frames is chosen with a calm face to calibrate the grimacing measure. This can be done by ensuring the measure was as constant as possible during a rotation of the head. Clinically, it would have to be done manually. Figure 7 shows the grimacing level as a function of the distance from the initial dot position before calibration. Also shown in Figure 7 is the best least squares fitted straight line. This line can be used to correct the grimacing measure using the formula:

$$\bar{G} = G - ax \quad (2)$$

where  $a$  is the gradient of the line in Figure 7,  $x$  the distance between the initial position and the current position of the white dot and  $G$  is the grimacing measure.

Thus, in summary, the position of the dot is used to correct unwanted changes that occur in the grimacing measure due to rotation of the head. Once the coefficient  $a$  is found, Equation (2) is applied to every image in the movie sequence. This process corrects the grimacing signal by returning a constant grimacing level during periods of calm in the patient.

Lastly, the grimacing measure is low pass filtered and normalized between 0 and 1 using a method similar to Equation (1). This step is important as it normalizes out any initial facial wrinkles in elderly patients, and other marks or scars present in the calm facial state. This approach ensures only the change from the calm state is measured which corresponds to a grimace.

### **3. Results**

#### **Reference point tracking – Step 1**

The black dot was successfully tracked throughout a 1336 frame (44.5 seconds) movie sequence, with the results of five frames shown in Figure 8, where the rectangle bounding the movement of the dot is also drawn. The left image shows the picture, while the right shows only the resulting binary image with the tracked dot. The rectangle is bigger in the first image because the position of the dot is unknown. After this initial frame the rectangle size is reduced. The white dot in the binary images of Figure 8 can be seen to accurately follow the position of the black dot, as denoted by a cross in the left image and thus the position of the head. The dot was successfully tracked for all 1336 frames with no lost or missed frames.

## **Extracting boundary contour of face – Step 2**

The contour of the face is tracked through a 1336 frame movie sequence, and 9 frames representing extreme cases are shown in Figure 9, with the extracted facial contours plotted in green. The boundary of the face was successfully tracked in all frames. As Figure 9 shows, the results are sufficiently accurate for this application, which requires only identification of the basic face area for further processing.

## **Facial grimacing (dynamic) – Steps 3-4**

The same 9 frames shown in Figure 9 are shown in Figure 10 with an agitation bar on the two sides of each image. The results show good consistency between the visually observed level of grimacing and the measured value shown on the bar is shown by the height of the panels to the left and right of the face in each image. The normalized level of grimacing is also plotted as a function of frame number in Figure 11; and consistent cycles can be seen that match the observed level of grimacing in Figure 10. Note that the number in each frame of Figure 10 are also shown in the plot of Figure 11 for added clarity. Finally, note that the qualitative levels and normalized quantitative assessments match well regardless of the rolling head motion that also occurs in the video.

## **4. Discussion and Conclusions**

This paper has investigated the image processing and feasibility of measuring the degree of facial grimacing in ICU patients using a single digital camera. The goal is to

develop methods for high-resolution measurement of changes in specific facial features that have been clinically observed to correlate with patient agitation and pain. Such a measure would enable more sensitive, quantitative, objective and accurate agitation assessment in critical care. Several simulations imitating a patient with differing degrees of grimacing and significant head movement are used to validate the approach.

Accurate position tracking was achieved with the artificial placement of a black dot locally surrounded by white. This dot can be placed either on the patients' forehead or on the ventilator tubing near the mouth. This dot is the only invasive feature of the overall approach.

To isolate the face an efficient algorithm was developed for tracking the overall facial contour based on skin hue and colour ratios. The cheek and eyebrows regions are used to detect agitation-based grimacing using edge detection methods. Good resolution was obtained for the normalized degree of grimacing measured and the results compared well to visually observed grimacing in the recorded images. Note that other methods, such as image surface roughness which could be measured using for example the fractal dimension [40,41], might also be used equally effectively.

In practice, any noise that occurs could be filtered leaving the essential dynamics required for this assessment. The orientation of the head could also be estimated to compensate for slight changes in the grimacing measure that occur due to the change in the angle of the camera as the head moves, particularly at extreme head rotations. Future experience with a number of critical care patients will allow a consistent angle correction factor to be chosen and other issues to be assessed.

The method can also be applied in real time as the computational time for processing 1 frame in Matlab 7.1, on a Pentium 4 with 3 GHz and 2 GB Ram, took

0.4 seconds. This is equivalent to 2.5 frames/s in Matlab, which is not real-time for a 30 fps application. However, reasonably optimized C code would provide a 10x-20x improvement, or 25 to 50 frames per second. Hence, the computational requirements are not too onerous for real-time application.

Future work will require clinical validation of the methods in this paper. In particular, direct comparison of the computed agitation level based on grimacing with agitation graded by nursing staff using the Riker Sedation-Agitation Scale or similar scale [30,31], will be required.

## References

[1] Kress, J. P., Pohlman, A. S., O'Connor, M. F., and Hall, J. B. (2000). Daily interruption of sedative infusions in critically ill patients undergoing mechanical ventilation, *N. Engl. J. Med.* 342(20):1471-1477.

[2] Burns AM, Shelly MP, Park GR. The use of sedative agents in critically ill patients. *Drugs* 1992; 43(4):507-15.

[3] J. Jacobi, Clinical practice guidelines for the sustained use of sedatives and analgesics in the critically ill adult, *Crit. Care Med.* 30 (1) (2002) 119-141.

[4] J.P. Wiener-Kronish, Problems with sedation and analgesia in the ICU, *Pulmonary Perspectives* 18(1) (2001).

[5] Andrew D. Rudge, "Modelling and control of Agitation-Sedation Dynamics in

Critically Ill Patients”, PhD thesis, University of Canterbury 2005.

[6] Chase, J G, Rudge, A D, Shaw, G M, Wake, G C, Lee, D, Hudson, I and Johnston, L (2004). “Modeling and Control of the Agitation-Sedation Cycle for Critical Care Patients,” *Medical Engineering and Physics*, 26(6): 459-471, ISSN: 1350-4533.

[7] Rudge, A. D., Chase, J. G., Shaw, G. M., Lee, D. S., Wake, G. C., Hudson, I.L., and Johnston, L. (2004). Impact of control on agitation/sedation dynamics. *Control Engineering Practice (CEP)*, Vol 13(9), pp. 1139-1149, ISSN: 0967-0661.

[8] Chase, J G, Starfinger, C, Lam, Z, Agogue, F and Shaw, G M (2004). "Quantifying Agitation in Sedated ICU Patients Using Heart Rate and Blood Pressure," *Physiological Measurement*, vol. 25, pp. 1037-1051, ISSN: 0967-3334

[9] Chase, J. G., Agogue, F. A., Starfinger, C., Lam, Z., Shaw, G. M., Rudge, A. D., and Sirisena, H. (2004a). Quantifying agitation in sedated ICU patients using digital imaging. *Computer Methods and Programs in Biomedicine*, 76(2):131-141.

[10] Agogue, F. A. (2005). Objective measurements of patient agitation in critical care using physiological signals and fuzzy systems. PhD thesis, University of Canterbury.

[11] A.D. Rudge, J.G. Chase, G.M. Shaw, D. Lee, (2006). Physiological modelling of agitation–sedation dynamics. *Medical Engineering & Physics* 28(1):49-59.

[12] Rudge, AD, Chase, JG, Shaw, GM and Lee, DS (2006). “Physiological Modelling of Agitation-Sedation Dynamics Including Endogenous Agitation Reduction,” *Medical Engineering and Physics*, 28(7):629-638 ISSN: 1350-4533.

[13] C. Weinert, L. Chlan, C. Gross, Sedating critically ill patients: factors affecting nurses’ delivery of sedative therapy, *Critic. Care* 10 (3) (2001) 156-167.

[14] Riker, R. R., Picard, J. T., and Fraser, G. L. (1999). Prospective evaluation of the sedation-agitation scale for adult critically ill patients. *Crit Care Med*, 27(7):1325-9.

[15] C. Sessler, M. Gosnell, M. Grap, G. Brophy, P. O’Neal, K. Keane, E. Tesoro, R. Elswick, The Richmond agitation-sedation scale: validity and reliability in adult intensive care unit patients, *Am J. Respir. Crit. Care Med.* 166 (2002) 1338—1344.

[16] [No authors listed] (2002). “Management of acute spinal cord injuries in an intensive care unit or other monitored setting,” *Neurosurgery*, 50(3 Suppl):S51-7.

[17] Bieri D, Reeve RA, Champion GD, Addicoat L, Ziegler JB (1990). "The Faces Pain Scale for the self-assessment of the severity of pain experienced by

children: development, initial validation, and preliminary investigation for ratio scale properties," *Pain*. 1990 May;41(2):139-50.

[18] Chambers CT, Giesbrecht K, Craig KD, Bennett SM, Huntsman E (1999). "A comparison of faces scales for measurement of pediatric pain: children's and parent's ratings," *Pain* 83:25–35

[19] Southall DP, Cronin BC, Hartmann H, et al (1993). "Invasive procedures in children receiving intensive care," *BMJ* 306:1512–13

[20] S C Maurice, J J O'Donnell and T F Beattie (2002). "Emergency analgesia in the paediatric population. Part I Current practice and perspectives," *Emerg Med J* 19:4-7

[21] Y Aissaoui, A A Zeggwagh, A Zekraoui, K Abidi and R Abouqal (2005). "Validation of a Behavioral Pain Scale in Critically Ill, Sedated, and Mechanically Ventilated Patients," *Anesth Analg* 101:1470-1476

[22] C Gelinas, M Fortier, C Viens, L Fillion and K Puntillo (2004). "Pain Assessment and Management in Critically Ill Intubated Patients: a Retrospective Study," *American Journal of Critical Care* 13: 126-136

[23] P K Dubey and A Kumar (2005). "Pain on Injection of Lipid-Free Propofol and Propofol Emulsion Containing Medium-Chain Triglyceride: A Comparative Study," *Anesth Analg* 101:1060-1062

[24] Kovach CR, Griffie J, Muchka S, Noonan PE, Weissman DE (2000). "Nurses' perceptions of pain assessment and treatment in the cognitively impaired elderly. It's not a guessing game," Clin Nurse Spec 14(5):215-20.

[25] Igier V, Mullet E, Sorum PC (2006). "How nursing personnel judge patients' pain," Eur J Pain, in press [Epub ahead of print]

[26] M. Kass, A. Witkin, and D. Terzopoulos, "Snakes: Active contour models," Int. J. Comput. Vis., vol. 1, pp. 321-331, 1987.

[27] K. Sobottka and I. Pitas, Segmentation and Tracking of Faces in Color Images, Second International Conference on Automatic Face and Gesture Recognition 1996, Killington, Vermont, USA, pp. 236-241, 14-16 October 1996.

[28] A. Jacquin and A. Eleftheriadis, "Automatic Location Tracking of Faces and Facial Features in Video Sequences", Proceedings, International Workshop on Automatic Face and Gesture Recognition, Zurich, Switzerland, June 1995.

[29] J. Tang and S.T. Acton, "Locating human faces in a complex background including non-face skin colors," Journal of Electronic Imaging, Vol.12, No.3, 2003.

[30] J. Tang and S.T. Acton, "A DCT based gradient vector flow snake for image segmentation", Proc. IEEE Southwest Symposium on Image Analysis and Interpretation, Lake Tahoe, Nevada, March 28-30, 2004

[31] Lanitis, A.; Taylor, C.J.; Cootes, T.F.; Automatic interpretation and coding of face images using flexible models, *Pattern Analysis and Machine Intelligence*, IEEE Transactions on Volume 19, Issue 7, July 1997 Page(s):743 – 756

[32] V. Vezhnevets, V. Sazonov, and A. Andreeva, "A survey on pixel-based skin color detection techniques," in *Proc. Graphicon-2003*.

[33] J. Brand and J. S. Mason. A Comparative Assessment of Three Approaches to Pixel level Human Skin-Detection. In *Proc of the International Conference on Pattern Recognition*, volume 1, pages 1056--1059, 2000.

[34] Soriano M, Martinkauppi B, Huovinen S & Laaksonen M (2000). "Skin detection in video under changing illumination conditions," *Proc. 15th International Conference on Pattern Recognition*, September 3-8, Barcelona, Spain, 1:839-842.

[35] M. Hunke, and A. Waibel (1994). "Face locating and tracking for human-computer interaction," *Proc. 28th Asilomar Conf. Signals, Systems and Computers* 2:1277-1281.

[36] M. Storrang, H. Andersen, E. Granum (1999). "Skin colour detection under changing lighting condition 7th Symposium on Intelligent Robotics Systems, 187-195,

[37] Filipe Tomaz and Tiago Candeias and Hamid Shahbazkia, Improved Automatic Skin Detection in Color Images, Proc. VIIth Digital Image Computing: Techniques and Applications, Sun C., Talbot H., Ourselin S. and Adriaansen T. (Eds.), 10-12 Dec. 2003, Sydney

[38] Rein-Lien Hsu; Abdel-Mottaleb, M.; Jain, A.K.; Face detection in color images, Pattern Analysis and Machine Intelligence, IEEE Transactions on Volume 24, Issue 5, May 2002 Page(s):696 – 706

[39] Marr D. and E. Hildreth, Theory of edge detection, Proc. R. Soc. Lond., 207:187-217 (1980).

[40] Jelinek, H.F., Cornforth, D.J., Roberts, A.J., Landini, G. and Bourke, P. (2004). Image Processing of Finite Size Rat Retinal Ganglion Cells using Multifractal and Local Connected Fractal Analysis, Lecture Notes in Computer Science, Springer-Verlag Heidelberg, Volume 3339, pp 961.

[41] Smith, J.T.G., Lange, G.D. and Marks, W.B. (1996). Fractal Methods and Results in Cellular Morphology - Dimensions, Lacunarity and Multifractals, Journal of Neuroscience Methods. 69 (1996) 123-136

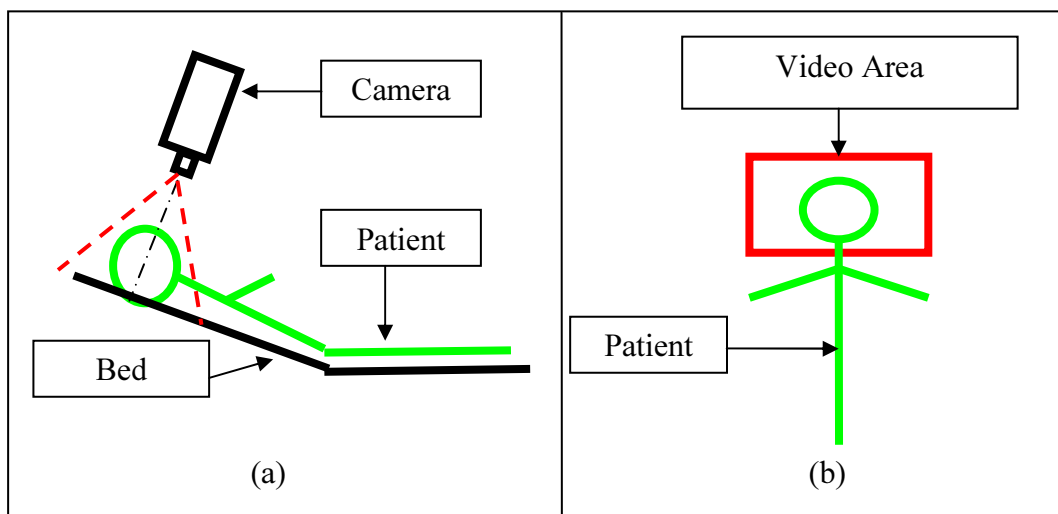


*Figure 1: Scheme of Experimental setup for video acquisition - (a) Side view - (b) Front view*

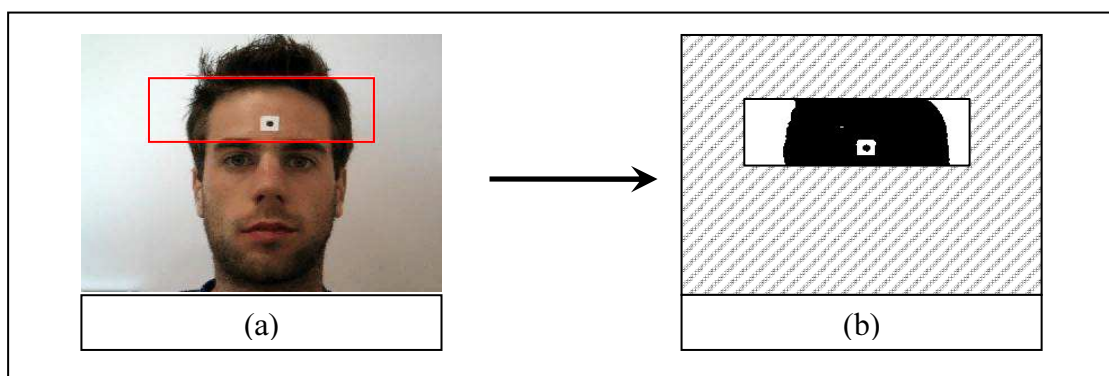


*Figure 2: (a) Original Jpeg image containing the analysed area; (b) Image of rectangle after doing a normalised thresholding*

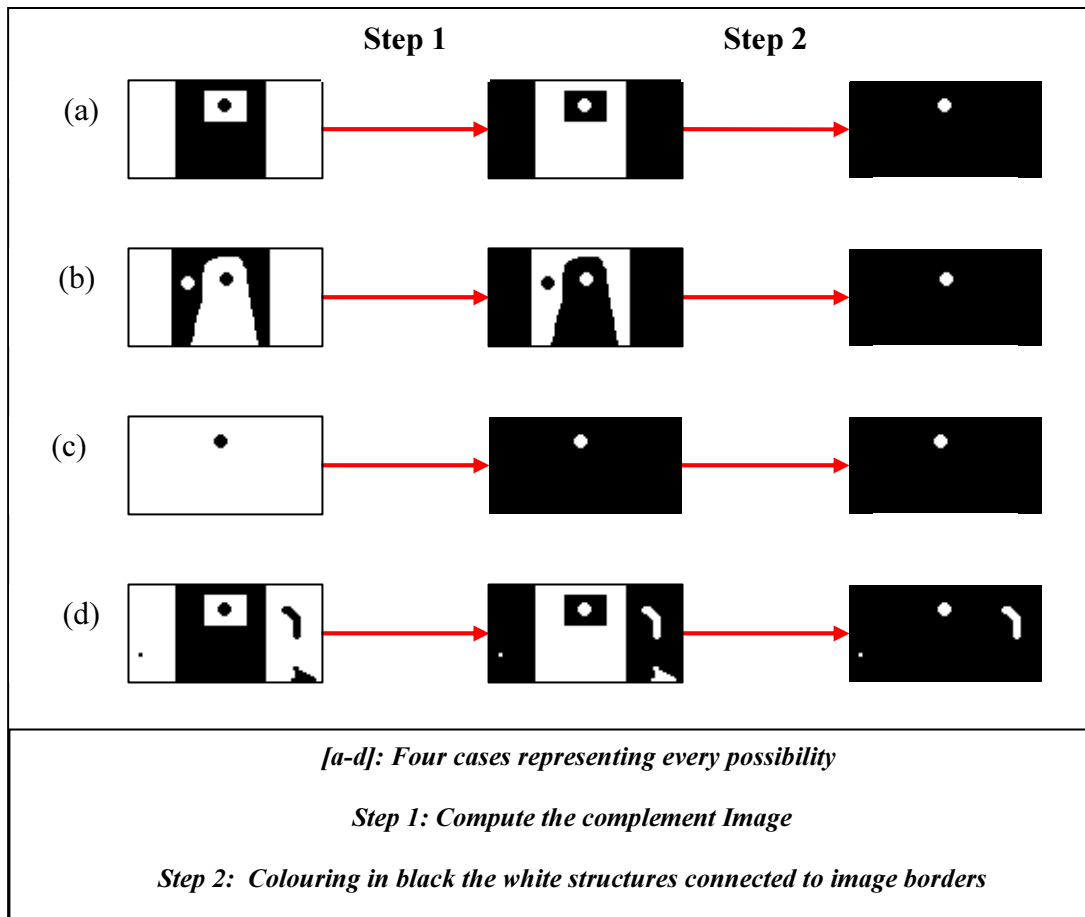


*Figure 3: Deleting unwanted regions to identify the required dot*

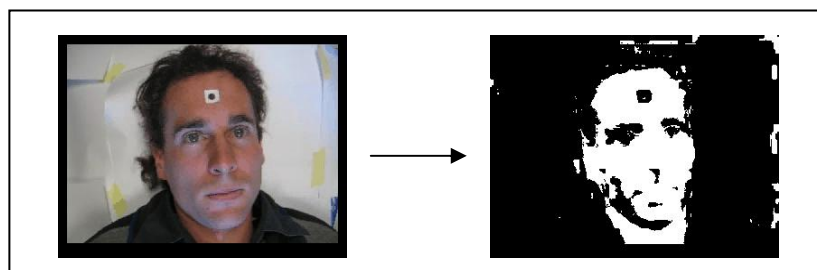


*Figure 4: Example of skin hue recognition*

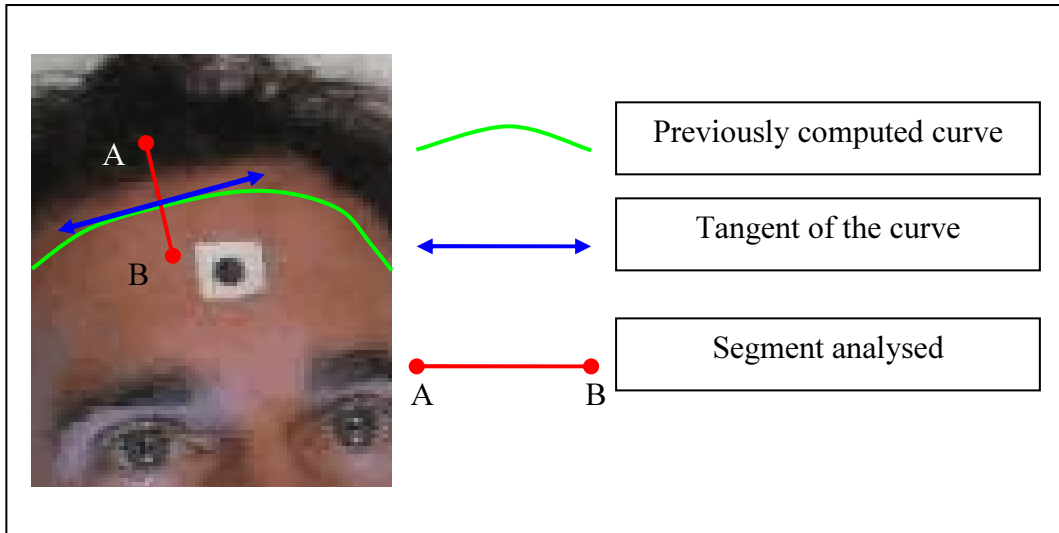


*Figure 5: Searching for new boundary within an envelope of the previous boundary.*

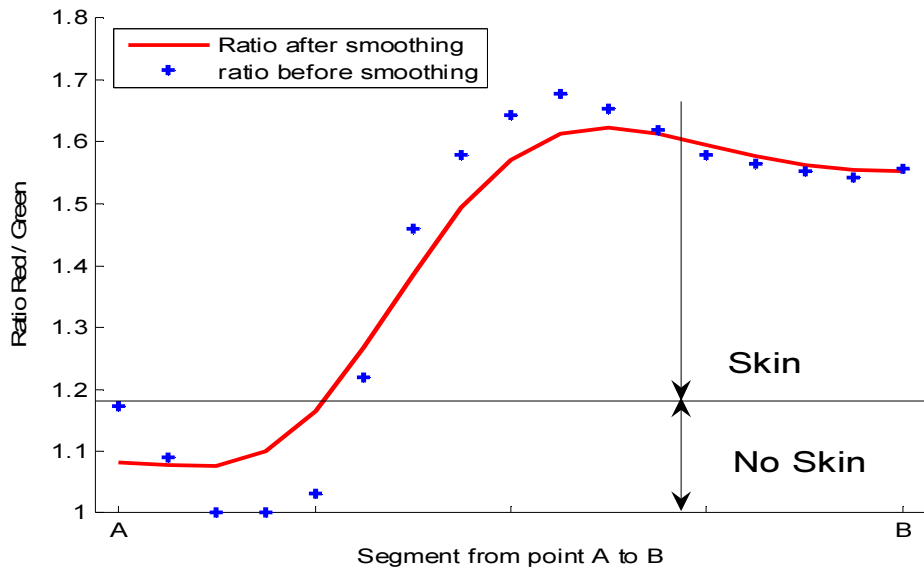


**Figure 6: Difference between Red and Green pixel intensity along the line A to B**

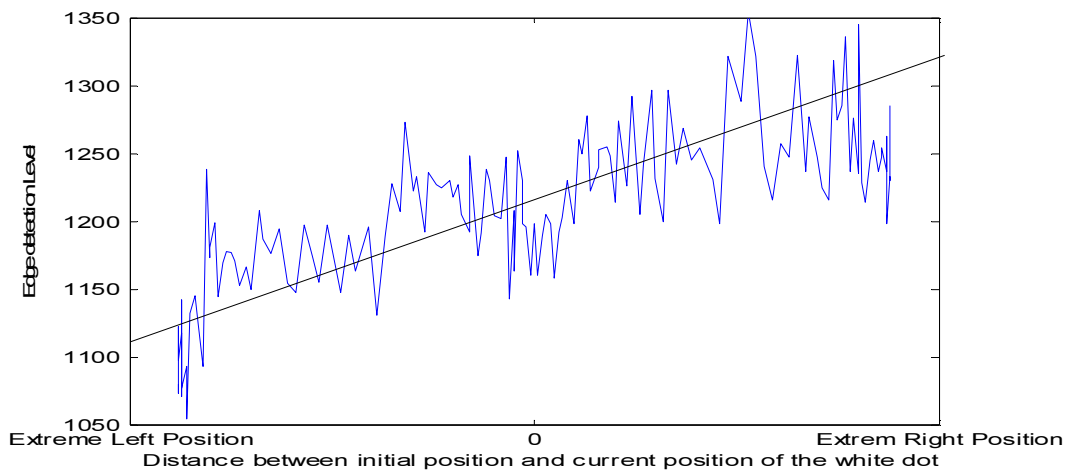


**Figure 7: Edge detection level in function of head position**

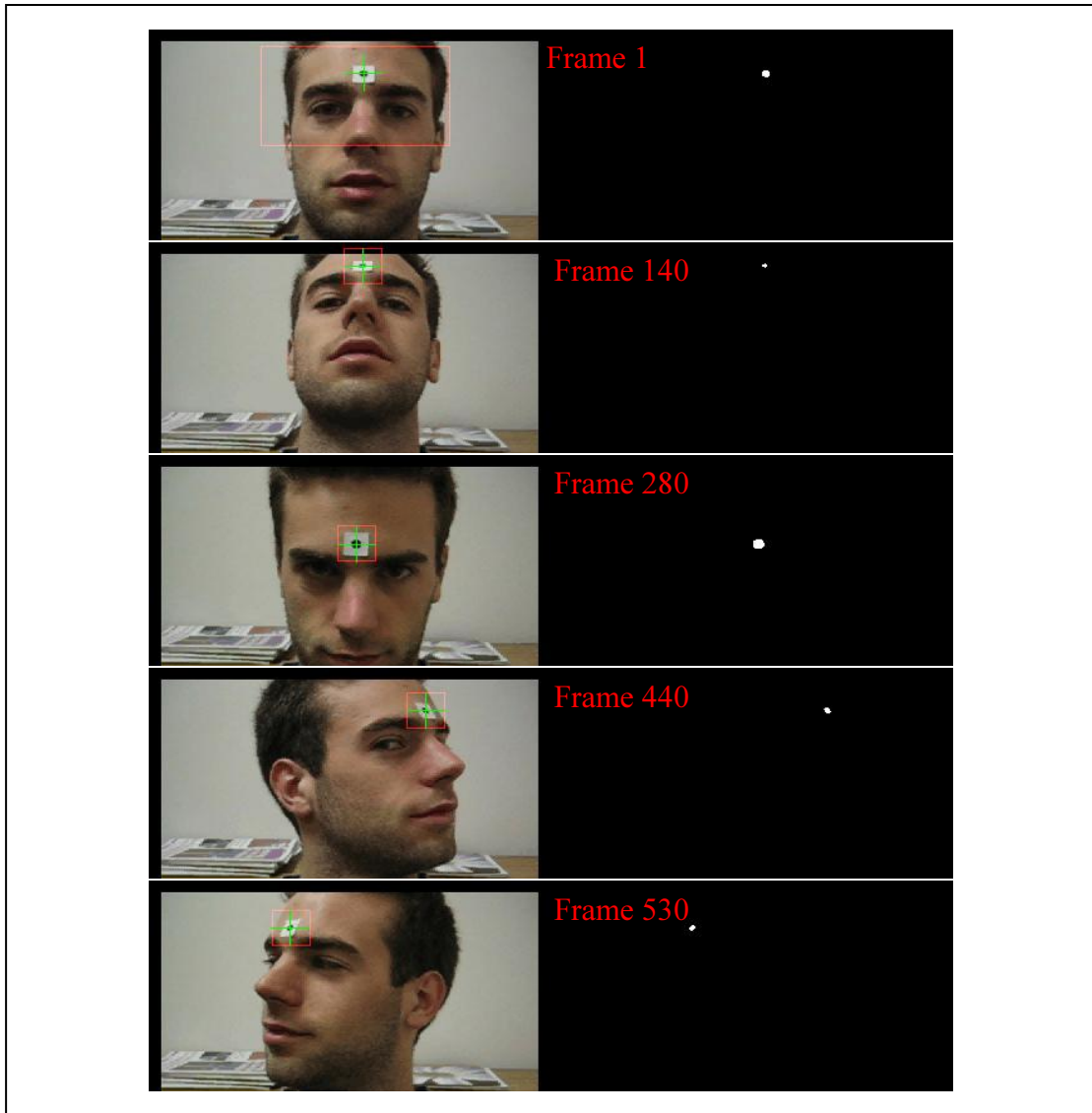


*Figure 8: Tracking the reference point throughout a movie sequence. Five frames, frame 1, 140, 280, 440 and 530 out of 1336 frames are shown, including the binary image of the dot.*

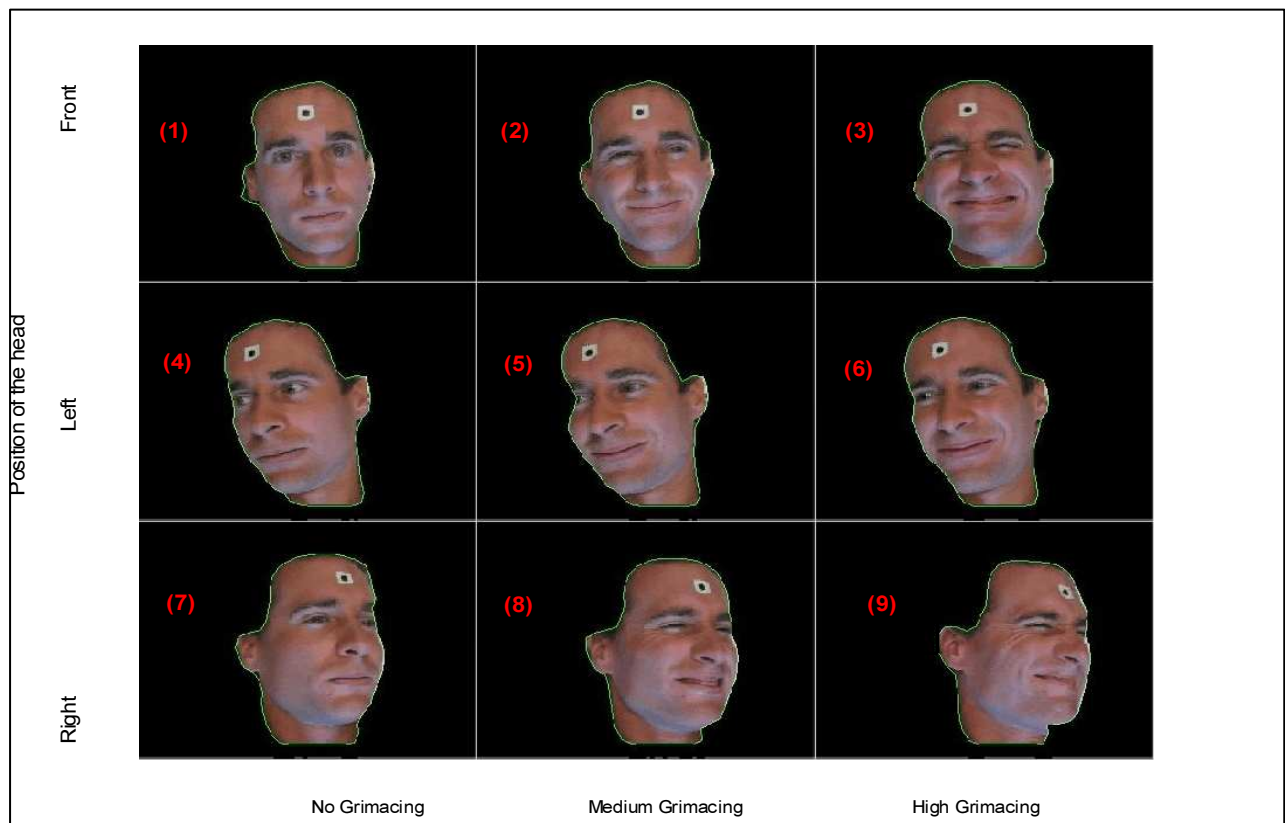


*Figure 9: Tracking face contour*



*Figure 10: Corresponding picture of the curve*

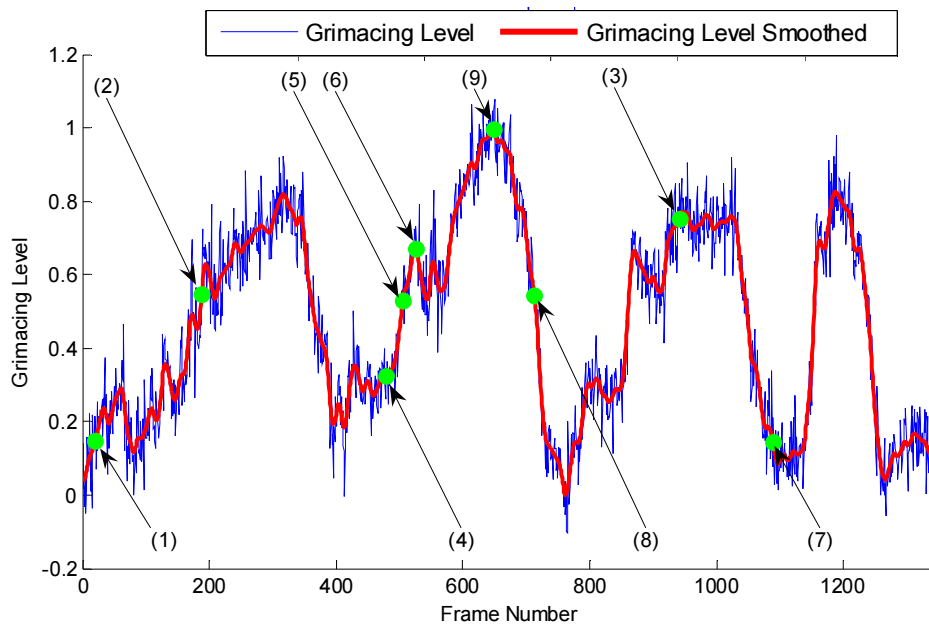


*Figure 11: Grimacing Measure (Dynamic) after angle correction*